J. Hydrol. Hydromech., 68, 2020, 3, 242–248
DOI: 10.2478/johh-2020-0020
ISSN 1338-4333

sciendo Journal of Hydrology and Hydromechanics

A new method for extracting spanwise vortex from 2D particle image velocimetry data in open-channel flow

Peng Zhang[1*], Shengfa Yang[2], Jiang Hu[2], Wenjie Li[2], Xuhui Fu[2], Danxun Li[1]

[1] State Key Laboratory of Hydroscience and Engineering, Tsinghua University, Beijing 100084, China.
[2] National Inland Waterway Regulation Engineering Research Center, Chongqing Jiaotong University, Chongqing 400074, China.
[*] Corresponding author. Tel.: +86 01062788532. Fax: +86 01062788532. E-mail: zpcquc@mail.tsinghua.edu.cn

Abstract: The two-dimensional particle image velocimetry (PIV) data are inevitably contaminated by noise due to various imperfections in instrumentation or algorithm, based on which the well-established vortex identification methods often yield noise or incomplete vortex structure with a jagged boundary. To make up this deficiency, a novel method was proposed in this paper and the efficiency of the new method was demonstrated by its applications in extracting the two-dimensional spanwise vortex structures from 2D PIV data in open-channel flows. The new method takes up a single vortex structure by combining model matching and vorticity filtering, and successfully locates the vortex core and draws a streamlined vortex boundary. The new method shows promise as being more effective than commonly used schemes in open-channel flow applications.

Keywords: Vortex identification; Spanwise vortex; Vorticity filtering; Open-channel flow.

INTRODUCTION

Turbulent flows, in both natural environments and engineering applications, involve various scales of motion which play an essential role in generation, distribution, and dissipation of turbulent energy as well as in transportation of mass, heat, and momentum (Adrian and Marusic, 2012; Chen et al., 2014a; Zhong et al., 2016). Among these multi-scale structures (Baidya et al., 2017; Jiménez, 2018), the vortex has long been recognized as a prominent feature in both closed-channel flow and open-channel flow (Dong et al., 2018; Zhong et al., 2017). Though a vortex still eludes precise definition (Kolář, 2007), it is generally held that 'a vortex exists when instantaneous streamlines mapped onto a plane normal to the vortex core exhibit a roughly circular or spiral pattern when viewed from a reference frame moving with the center of the vortex core'(Robinson, 1991). Vortical regions in various turbulent flows are unanimously characterized by high vorticity, low pressure, and compact streamline (Epps, 2017). In open-channel flows, the vortex in the streamwise-wall-normal plane, called a spanwise vortex, attracts enormous attention due to its importance in momentum convection and the convenience in experimental observation.

Extraction of the spanwise vortex from background turbulence can be achieved based on either local or global information of the velocity field. Local approaches of vortex identification employ a specific point-wise indicator to determine whether that point falls inside/outside a vortex. Global approaches, on the other hand, examine the overall topological feature of the flow to draw the boundary of a vortex.

Earlier local vortex extraction methods used vorticity as a point-wise indicator. To eliminate the contamination of shear effect (Cucitore et al., 1999; Kolář, 2010), recent local approaches turn to other indicators based the velocity gradient tensor, e.g., Δ (Chong et al., 1990), Q (Hunt et al., 1988), λ_2 (Jeong and Hussain, 1995), λ_{ci} (Zhou et al., 1999), and Ω (Liu et al., 2016; Zhang et al., 2018). While these indicators are useful in quantifying vortex strength, it is still difficult to select a proper universal threshold for them in non-uniform flows where vortices exhibit a broad spectrum of variation in size and strength, e.g., a higher value may lead to blurring of weaker vortices, and conversely, a lower one may result in cluttering of stronger vortices (Dong et al., 2016). Such difficulty has been partially overcome by normalization of the average indicator with its root-mean-square in cases where enough samples of the flow are available for statistical analysis (Cao et al., 2017; Chen et al., 2014b; Wu and Christensen, 2006; Zhong et al., 2015). In experimental studies, another disadvantage of the local-based vortex extraction methods becomes evident: a small change in spatial resolution may induce significant deviation in vortex identification (Gao et al., 2011).

Global methods offer a more intuitive approach to extracting vortex. For example, through pattern-recognition and model-matching technique, a vortex is recognized by fitting the target flow against a standard model (Chen et al., 2013; Stanislas et al., 2008). Note that global methods for vortex extraction are on the dependence of the transitional velocity of an observer (Cucitore et al., 1999). While simple and straightforward in concept, the global methods suffer from limitations due to the arbitrariness in selecting reference frames, model vortex, and other subjective parameters.

A combination of the advantages of local and global approaches provides a new way to enhance the effectiveness of vortex extraction. Dong et al. (2016), for instance, developed a λ_2-scheme coupled with vortex filaments and accurately found the vortex structure. Unfortunately, this method cannot be used for identifying spanwise vortex as calculation of the vortex filaments is impossible in the two-dimensional velocity field.

Extraction of a spanwise vortex in open-channel flows further complicated by the coexistence of shear and rotation, the interaction between various structures, the influence of channel bed and water surface (Roussinova et al., 2010; Zhang et al., 2015), and the variation of a vortex in size, shape, and strength (Hurther et al., 2007; Komori et al., 1989). This is particularly true when PIV data are used for vortex analysis (Singha and Balachandar, 2011). Though PIV has long been used as an

efficient and effective fluid velocity measurement technique, the measured data are inevitably contaminated by noise due to various imperfections in instrumentation or algorithm, e.g., limited interpretation window, uneven distribution of tracer particles, and non-uniformity in light intensity of the laser sheet. Based on such measurement data, well-established vortex methods often yield incomplete vortex structures with a jagged boundary (Nezu and Sanjou, 2011). Precise quantification of a spanwise vortex in open-channel flows necessitates the development of a novel extraction method.

The present paper proposes a novel vortex extraction method by combining model matching and vorticity filtering for a single vortex structure. For analysis of vortex structure based on PIV data, the new method shows a better adaptation to vortex strength, a more precise and streamlined delineation of vortex boundary, and enhanced accuracy in portraiting vortex structure.

NEW EXTRACTING METHOD FOR A SINGLE VORTEX STRUCTURE

The new identification algorithm, which combines the techniques of model matching and vorticity filtering, follows a series of steps as described below.

Step 1. Locating the vortex core.

The core of a vortex can be found by examining the fluctuating flow velocity in its surrounding grid nodes, as shown in Fig. 1, where (i, j) represents the center of a vortex, either prograde (Fig. 1a) or retrograde (Fig. 1b). Note that the fluctuating velocity is derived from Reynolds decomposition, which has been proven to be useful for vortex visualization (Carlier and Stanislas, 2005).

A vortex core is recognized if the following conditions are satisfied (Chen et al., 2013),

$$\begin{cases} u'(i-1,j)<0, u'(i+1,j)>0 \\ v'(i,j-1)>0, v'(i,j+1)<0 \end{cases}, \text{ as a prograde vortex,} \tag{1}$$

and

$$\begin{cases} u'(i-1,j)>0, u'(i+1,j)<0 \\ v'(i,j-1)<0, v'(i,j+1)>0 \end{cases}, \text{ as a retrograde vortex,} \tag{2}$$

where u' and v' represent streamwise and wall-normal fluctuation velocity, respectively. Note that zero velocity is expected at a real vortex centroid. The reason why the criterion involves no requirement at (i, j) lies in that it is tough for a vortex core with zero velocity to fall precisely to a grid node in practical measurement. The relaxation of restrictions may lead to the presence of two or more neighboring nodes competing for a vortex core. In such cases, the point with the least velocity is chosen as the vortex core among all the candidates, denoted as (m, n).

Step 2. Calculating vorticity in an area around the vortex core.

The choice of vorticity as a vortex indicator will be discussed in the subsequent section.

A square or rectangle centered at an identified vortex core is used to enclose a specific area where a vortex may exist, denoted as D_{IJ},

$$D_{IJ} = \left\{ (I,J) \middle| \begin{matrix} I \in [m-\Delta m, \ldots, m, \ldots, m+\Delta m] \\ J \in [n-\Delta n, \ldots, n, \ldots, n+\Delta n] \end{matrix} \right\} \tag{3}$$

where Δm and Δn are integers that specify half the size of the target area in x (streamwise) and y (wall-normal) directions, respectively, and their values can be estimated based on the size of spanwise vortex structure.

Vorticity matrix on D_{IJ} is given as follows,

$$\omega_D = \begin{pmatrix} \omega_{1,1} & \cdots & \omega_{1,l} & \cdots & \omega_{1,2\Delta n+1} \\ \vdots & \vdots & \vdots & \vdots & \vdots \\ \omega_{k,1} & \cdots & \omega_{k,l} & \cdots & \omega_{k,2\Delta n+1} \\ \vdots & \vdots & \vdots & \vdots & \vdots \\ \omega_{2\Delta m+1,1} & \cdots & \omega_{2\Delta m+1,l} & \cdots & \omega_{2\Delta m+1,2\Delta n+1} \end{pmatrix}, \tag{4}$$

where $k \in [1, \ldots, 2\Delta m+1]$, $l \in [1, \ldots, 2\Delta n+1]$, and,

$$\omega_{D,IJ} = \frac{1}{2}\left(\frac{\partial u'}{\partial y} - \frac{\partial v'}{\partial x} \right), \tag{5}$$

where u', v' are streamwise and wall-normal fluctuating velocities, respectively.

Step 3. Vorticity filtering.

A two-dimensional template, ω_T, is used for vorticity filtering,

$$\omega_T = \begin{pmatrix} \omega_{1,1} & \cdots & \omega_{1,j} & \cdots & \omega_{1,nj} \\ \vdots & \vdots & \vdots & \vdots & \vdots \\ \omega_{i,1} & \cdots & \omega_{i,j} & \cdots & \omega_{i,nj} \\ \vdots & \vdots & \vdots & \vdots & \vdots \\ \omega_{ni,1} & \cdots & \omega_{ni,j} & \cdots & \omega_{ni,nj} \end{pmatrix} \tag{6}$$

where $i \in [1, \ldots, ni]$, $j \in [1, \ldots, nj]$, ni and nj are odd numbers (thus setting a vortex core exactly at center). In practice, a proper ω_T can be chosen based on the averaged flow field, as will be discussed in the subsequent section.

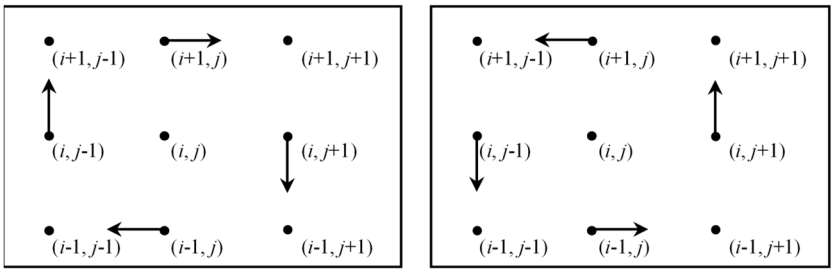

(a) prograde vortex (b) retrograde vortex

Fig. 1. Spanwise vortex core model (Chen et al., 2013).

Matrix expression of the enhanced vorticity distribution, ω_{post}, is as follows,

$$\omega_{post}(k,l)=\sum_{j=1}^{nj}\sum_{i=1}^{ni}\left(\omega_T(i,j)\times\omega_D\left(k-\frac{ni+1}{2}+i,l-\frac{nj+1}{2}+j\right)\right), \quad (7)$$

where $k\in[1, \ldots, 2\Delta m+1]$, $l\in[1, \ldots, 2\Delta n+1]$. For the edge of the measured velocity field, zero paddings are used to ensure calculation.

To facilitate the determination of a universal threshold for the entire flow, the enhanced vorticity is further normalized by its maximum absolute value as follows,

$$\omega'_{post}=\frac{1}{|\omega_{post}|_{max}}\omega_{post},\ \omega'_{post}\in[-1, 1], \quad (8)$$

The nodes in D_{IJ} at which ω'_{post} is above the threshold are recognized as within a vortex. The determination of the thresh old will be discussed in the subsequent section.

SIZE OF FILTER TEMPLATE AND THRESHOLD OF VORTICITY

Effectiveness of vorticity as a vortex indicator

Observation of open-channel flow reveals that vorticity is a valid indicator to display the spatial scope of a vortex. This is illustrated in Fig. 2, which shows two typical velocity fields obtained from open-channel flow PIV measurement, one with a prograde vortex and the other a retrograde one. Streamwise fluctuation velocity along the y-axis and wall-normal fluctuation velocity along the x-axis are indicated with red lines in Fig. 2. Typical vortical flows characterize the velocity distribution, i.e., it remains zero at vortex core, begins to increase along the axis, reaches maximum somewhere, and then turns to drop. As a minimum requirement, an effective vortex extraction scheme needs to recognize at least the core vortex region extending to the maximum velocity.

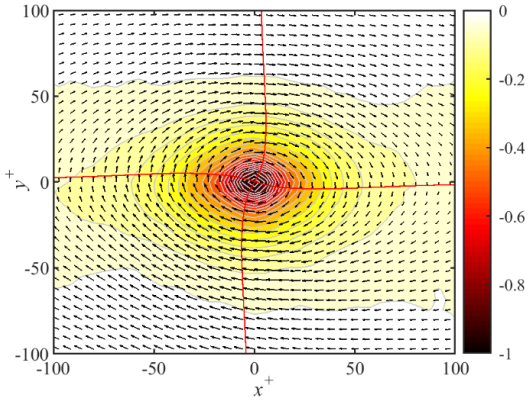

(a) vorticity distribution of prograde vortex

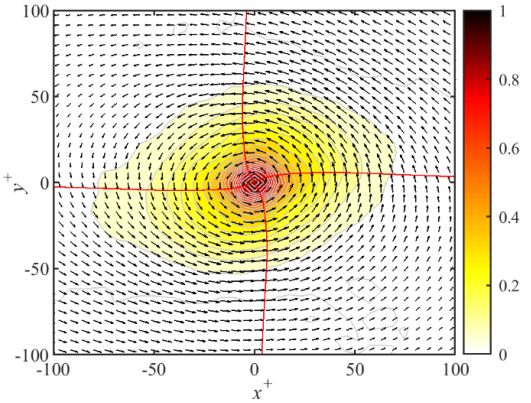

(b) vorticity distribution of retrograde vortex

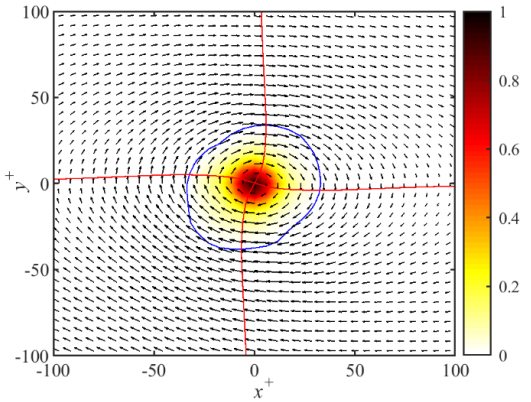

(c) Q method of prograde vortex

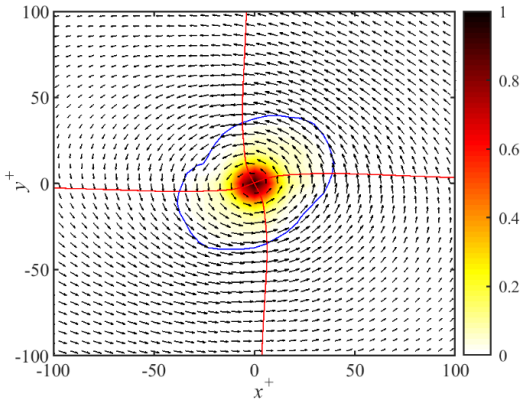

(d) Q method of retrograde vortex

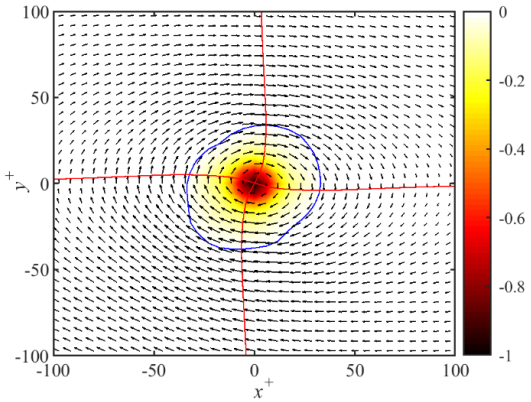

(e) λ_2 method of prograde vortex

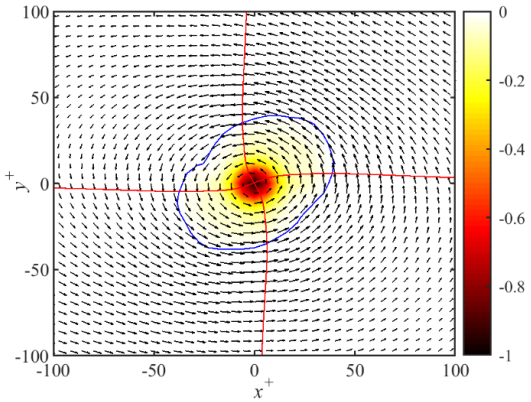

(f) λ_2 method of retrograde vortex

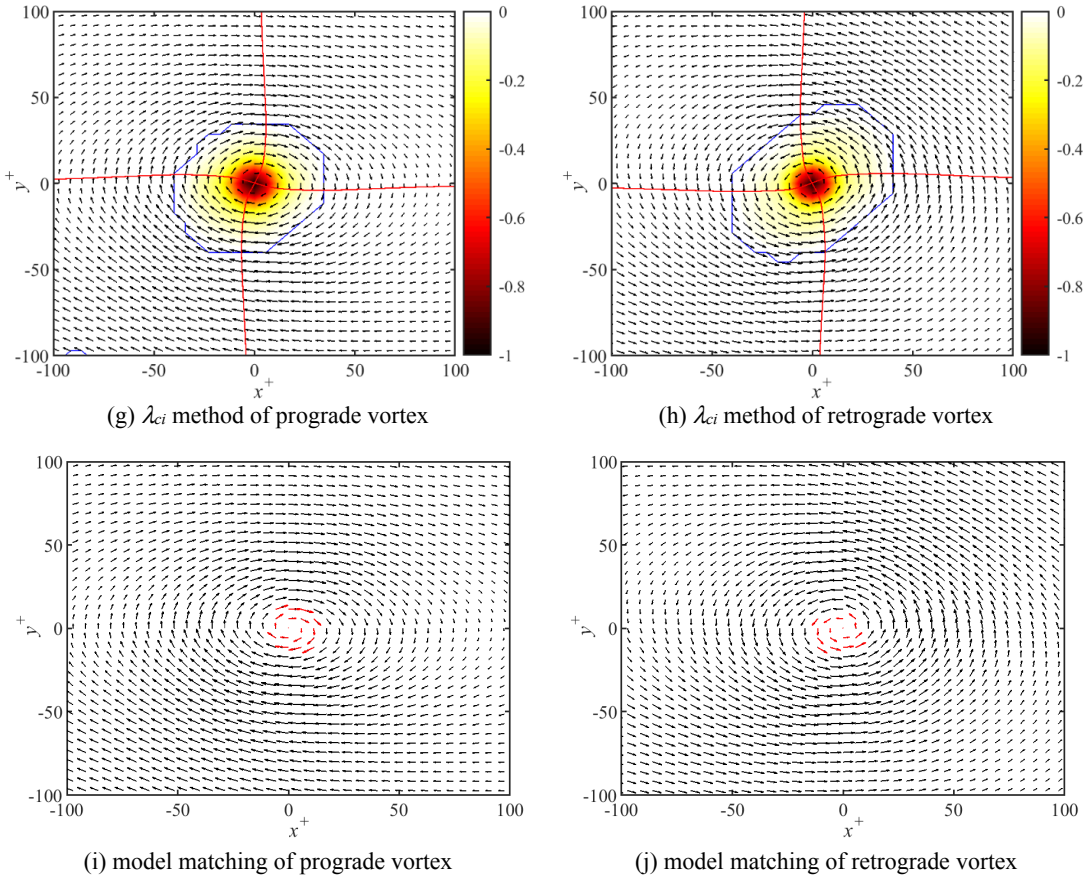

(g) λ_{ci} method of prograde vortex (h) λ_{ci} method of retrograde vortex

(i) model matching of prograde vortex (j) model matching of retrograde vortex

Fig. 2. Vortex regions identified by different methods.

Fig. 2 also shows the vortex extraction results based on vorticity, Q, λ_2, λ_{ci} (all after normalization) with a universal threshold of zero. The result by pattern recognition is also included. The analysis is based on a PIV database of the turbulent open-channel flow by Yang et al., (2016). The C case is selected and introduced briefly here. The case is uniform flow in a smooth open-channel, where the slope, water depth, aspect ratio, bulk mean velocity, friction velocity viscous length scales, and friction Reynolds number are 0.0015, 33 mm, 7.56, 0.41 m/s, 0.022 m/s, 0.045 mm, 574, respectively.

It is seen that the identified vortex with vorticity (Fig. 2a, b), Q (Fig. 2c, d), λ_2 (Fig. 2f), and λ_{ci} (Fig. 2g, h), elliptical or circular, exhibits a length scale (radius) of 100,40, 40 and 40 y_* ($y_* = \nu/u_*$ is the viscous length scales, ν is kinematic viscosity, u_* = friction velocity), respectively. All methods successfully identify the core vortex region. Clearly, vorticity is the most effective indicator for determining the vortex spatial scope. The pattern recognition method (Fig. 2i, j), however, failed to extract a vortex of a reasonable size.

Determination of the filter template's size

The choice of a proper filter template is of principal importance for vortex extraction in open-channel flows where flow structures are complicated by the presence of sidewalls, free surface, and bed slope. In general, a proper filter template for prograde or retrograde vortices can be easily constructed based on the average over respective vorticity fields. Determination of the size for a filter template, as well, evolves experience-based knowledge. According to previous studies on averaged spanwise vortex structure (Adrian et al., 2000; Natrajan et al., 2007; Singha and Balachandar, 2011), its core spans a range of 30–50y_*; its vorticity decreases from peak to zero in the range of 100–150y_*.

Fig. 3 shows typical prograde and retrograde vortices at a mesh of 250y_* × 250y_*, with corresponding elliptical streamlines. Against these flow fields, a comparison of the vortex extraction performance of the new method has been done by varying the filter template size, with a mesh of 150y_* × 150y_*, 200y_* × 200y_*, 250y_* × 250y_*, respectively. The probability distribution functions (pdf) of ω'_{post} are shown in Fig. 4.

It is seen that the probability distribution functions grow 'taller and thinner' as the size of the filter template decreases. In the interval of (0.4, 1), however, the influences of the template size become negligibly small. Thus, the value of 0.4 can be used as a threshold. Thought the filter template size seems to exert no influence on the vorticity threshold, it also plays an important role, e.g., an increase in size leads to uniformization of the vorticity field in a weakly rotating region and a reduction causes a concentration of the vorticity field. Therefore, a recommended size for the filter template is 200y_* × 200y_*, which is slightly larger than the average size of the spanwise vortex structure reported by previous studies (Adrian et al., 2000; Natrajan et al., 2007; Singha and Balachandar, 2011).

PERFORMANCE TEST OF THE NEW METHOD

The suitability of the novel method has been tested against experimental data obtained with PIV in a fully developed turbulent open-channel flow. Detailed information on the experimental setup, measurement technique, and data description can be found in Yang et al. (2016). Comparison has also been made with the vorticity and λ_{ci} methods.

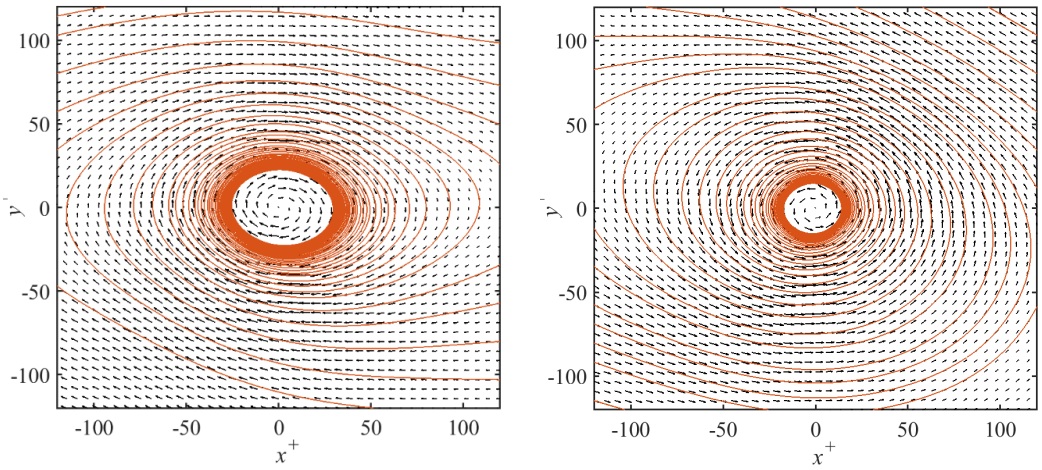

(a) prograde vortex (b) retrograde vortex

Fig. 3. Streamlines of prograde and retrograde vortex.

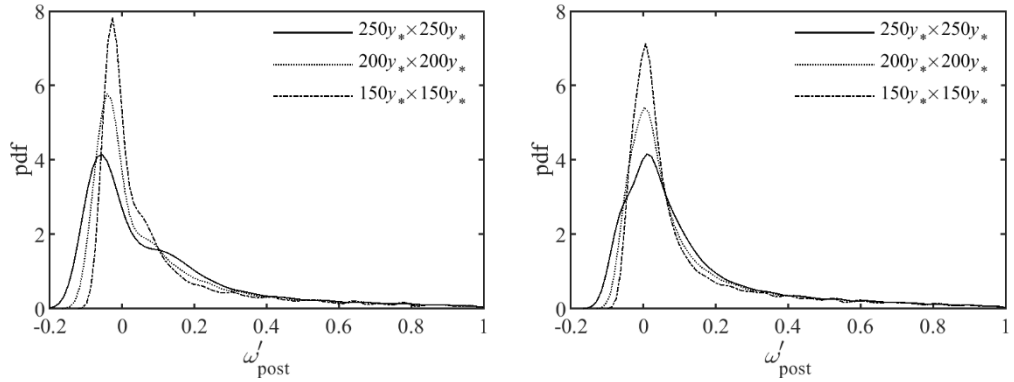

(a) prograde vortex (b) retrograde vortex

Fig. 4. The probability distribution functions (pdf) of the prograde and retrograde vortex.

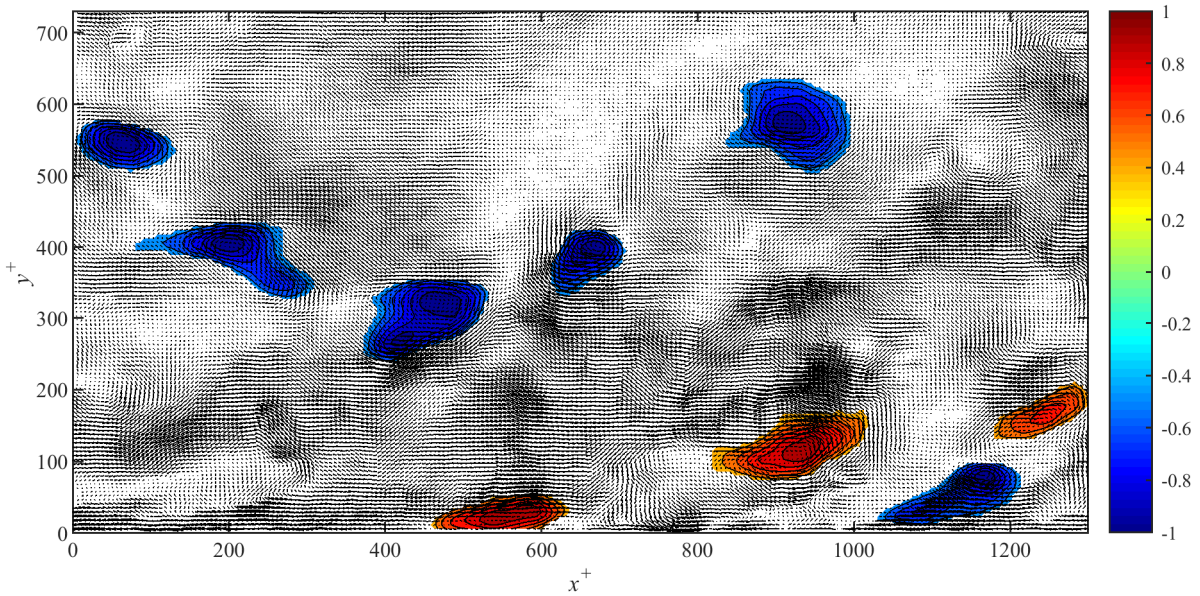

Fig. 5. The distribution of spanwise vortex structures identified by the new method.

Fig. 5 shows the detection results of the new method (blue and red regions represent prograde and retrograde vortex, respectively). An examination of the flow field indicates that all vortices are successfully identified with the new method, and every vortex has a clear and streamlined boundary.

The difference between different methods becomes evident when one takes a closer look at the vortex centered at (200, 400) and (940, 120), as shown in Fig. 6, where the contour lines indicate the vortex structure identified by the new method. The contrast shows a plaque-like vortex by the

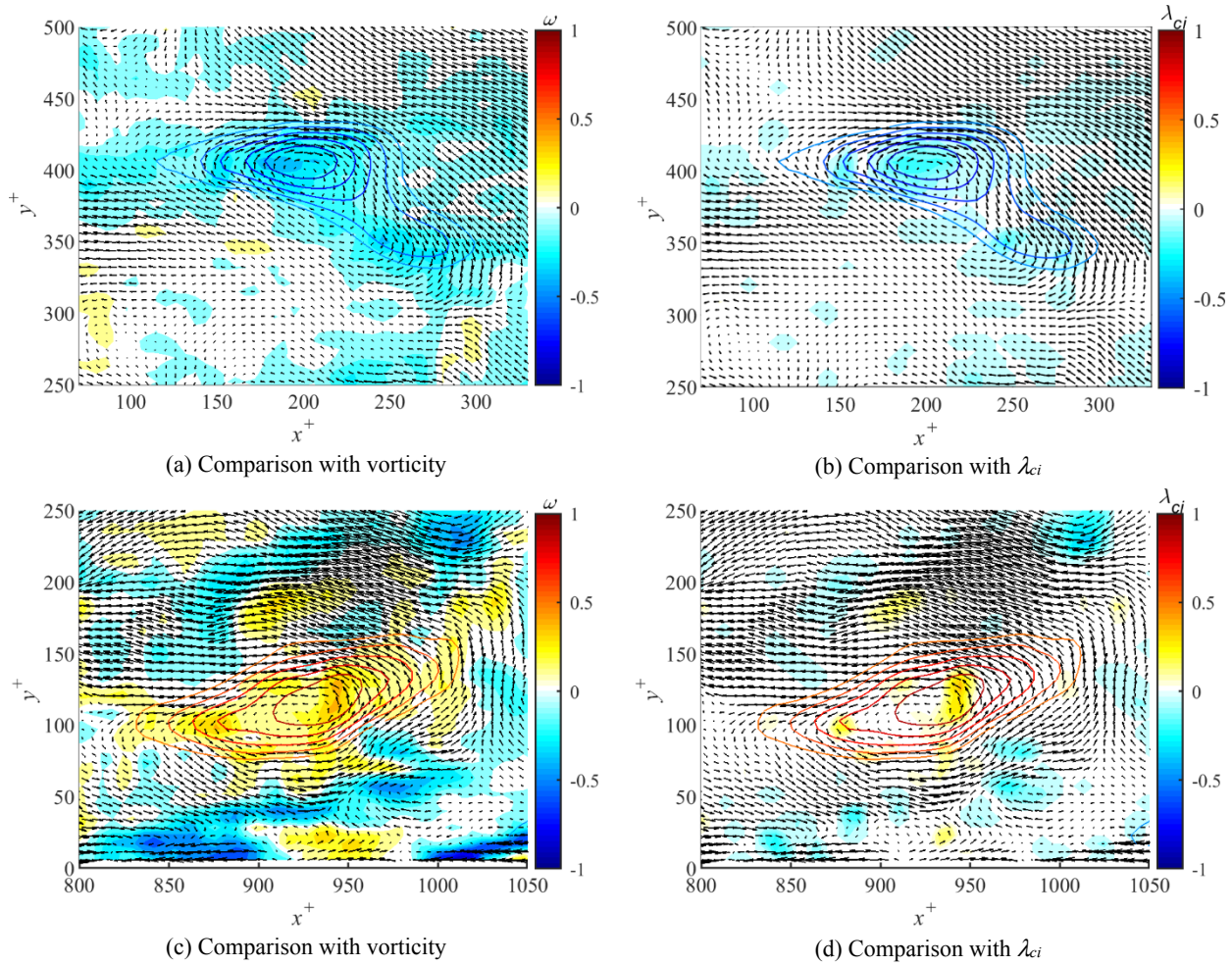

Fig. 6. Different spanwise vortex ranges identified by the new method, vorticity, λ_{ci} method.

vorticity approach (Fig. 6a, c), and small vortex 'patches' by the λ_{ci} method (Fig. 6b, d). As expected, the vortices extracted with the new method show good agreement with the real flow.

CONCLUSIONS

The present paper proposes a novel method for two-dimensional spanwise vortex identification from 2D PIV data in open-channel flows. Compared with existing schemes, the new method can adequately account for the differences of a vortex in strength and size. Thus a streamlined description of the integrity of vortex structures becomes possible. Major conclusions are summarized as follows:

(1) A combination of model matching and vorticity filtering is useful for accurately determining a vortex core.

(2) Vorticity has been proven to be a valid indicator of the spatial scope of a vortex. Normalization by the maximum value facilitates the determination of an appropriate threshold.

(3) The size of the prograde/retrograde vortex filter template is recommended as $200y_* \times 200y_*$, which is slightly larger than the average size of the spanwise vortex structure.

Acknowledgements. The study is financially supported by the National Natural Science Foundation of China (No. 51679020) and the National Key Research and Development Program of China (No. 2018YFB1600400).

REFERENCES

Adrian, R.J., Marusic, I., 2012. Coherent structures in flow over hydraulic engineering surfaces. Journal of Hydraulic Research, 50, 451–464.

Adrian, R.J., Meinhart, C.D., Tomkins, C.D., 2000. Vortex organization in the outer region of the turbulent boundary layer. Journal of Fluid Mechanics, 422, 1–54.

Baidya, R., Philip, J., Hutchins, N., Monty, J.P., Marusic, I., 2017. Distance-from-the-wall scaling of turbulent motions in wall-bounded flows. Physics of Fluids, 29, 020712.

Cao, L.K., Li, D.X., Chen, H., Liu, C.J., 2017. Spatial relationship between energy dissipation and vortex tubes in channel flow. Journal of Hydrodynamics, 29, 575–585.

Carlier, J., Stanislas, M., 2005. Experimental study of eddy structures in a turbulent boundary layer using particle image velocimetry. Journal of Fluid Mechanics, 535, 143–188.

Chen, Q.G., Li, D.X., Zhong, Q., Wang, X.K., 2013. Analysis of vortex structure in open channel turbulence based on model matching. Advances in Water Science, 24, 95–102. (In Chinese.)

Chen, Q.G., Adrian, R.J., Zhong, Q., Li, D.X., Wang, X.K., 2014a. Experimental study on the role of spanwise vorticity and vortex filaments in the outer region of open-channel flow. Journal of Hydraulic Research, 52, 476–489.

Chen, Q.G., Zhong, Q., Wang, X.K., Li, D.X., 2014b. An improved swirling-strength criterion for identifying

spanwise vortices in wall turbulence. Journal of Turbulence, 15, 71–87.
Chong, M.S., Perry, A.E., Cantwell, B.J., 1990. A general classification of three-dimensional flow fields. Physics of Fluids A, 2, 765–777.
Cucitore, R., Quadrio, M., Baron, A., 1999. On the effectiveness and limitations of local criteria for the identification of a vortex. European Journal of Mechanics, B/Fluids, 18, 261–282.
Dong, X., Wang, Y., Chen, X., Dong, Y., 2018. Determination of epsilon for Omega vortex identification method. Journal of Hydrodynamics, 30, 541–548.
Dong, Y., Yan, Y., Liu, C., 2016. New visualization method for vortex structure in turbulence by lambda2 and vortex filaments. Applied Mathematical Modelling, 40, 500–509.
Epps, B., 2017. Review of Vortex Identification Methods. In: 55th AIAA Aerospace Sciences Meeting. American Institute of Aeronautics and Astronautics, Texas, p. 0989.
Gao, Q., Ortiz-Dueñs, C., Longmire, E.K., 2011. Analysis of vortex populations in turbulent wall-bounded flows. Journal of Fluid Mechanics, 678, 87–123.
Hunt, J.C.R., Wray, A.A., Moin, P., 1988. Eddies, streams, and convergence zones in turbulent flows. In: Center for Turbulence Research Report, pp. 193–208.
Hurther, D., Lemmin, U., Terray, E.A., 2007. Turbulent transport in the outer region of rough-wall open-channel flows: The contribution of large coherent shear stress structures (LC3S). Journal of Fluid Mechanics, 574, 465–493.
Jeong, J., Hussain, F., 1995. On the identification of a vortex. Journal of Fluid Mechanics, 285, 69–94.
Jiménez, J., 2018. Coherent structures in wall-bounded turbulence. Journal of Fluid Mechanics, 842, P1.
Kolář, V., 2007. Vortex identification: New requirements and limitations. International Journal of Heat and Fluid Flow, 28, 638–652.
Kolář, V., 2010. A note on integral vortex strength. Journal of Hydrology and Hydromechanics, 58, 23–28.
Komori, S., Murakami, Y., Ueda, H., 1989. The relationship between surface-renewal and bursting motions in an open-channel flow. Journal of Fluid Mechanics, 203, 103–123.
Liu, C.Q., Wang, Y.Q., Yang, Y., Duan, Z.W., 2016. New omega vortex identification method. Science China: Physics, Mechanics and Astronomy, 59, 684711.
Natrajan, V.K., Wu, Y., Christensen, K.T., 2007. Spatial signatures of retrograde spanwise vortices in wall turbulence. Journal of Fluid Mechanics, 574, 155–167.
Nezu, I., Sanjou, M., 2011. PIV and PTV measurements in hydro-sciences with focus on turbulent open-channel flows. Journal of Hydro-Environment Research, 5, 215–230.
Robinson, S.K., 1991. Coherent motions in the turbulent boundary layer. Annual Review of Fluid Mechanics, 23, 601–639.
Roussinova, V., Shinneeb, A.-M., Balachandar, R., 2010. Investigation of fluid structures in a smooth open-channel flow using proper orthogonal decomposition. Journal of Hydraulic Engineering, 136, 143–154.
Singha, A., Balachandar, R., 2011. Coherent structure statistics in the wake of a sharp-edged bluff body placed vertically in a shallow channel. Fluid Dynamics Research, 43, 055504.
Stanislas, M., Perret, L., Foucaut, J.M., 2008. Vortical structures in the turbulent boundary layer: A possible route to a universal representation. Journal of Fluid Mechanics, 602, 327–382.
Wu, Y., Christensen, K.T., 2006. Population trends of spanwise vortices in wall turbulence. Journal of Fluid Mechanics, 568, 55–76.
Yang, S.F., Zhang, P., Hu, J., Li, W.J., Chen, Y., 2016. Distribution and motion characteristics of Q-events for open-channel uniform flow. Advances in Water Science, 27, 430–438. (In Chinese.)
Zhang, P., Yang, S.F., Hu, J., Chen, Y., Xin, Y., 2015. Distribution of motion scales of vortices in turbulent open channel flow. Advances in Water Science, 26, 91–98. (In Chinese.)
Zhang, Y., Qiu, X., Chen, F., Liu, K., 2018. A selected review of vortex identification methods with applications. Journal of Hydrodynamics, 30, 767–779.
Zhong, Q., Li, D.X., Chen, Q.G., Wang, X.K., 2015. Coherent structures and their interactions in smooth open channel flows. Environmental Fluid Mechanics, 15, 653–672.
Zhong, Q., Chen, Q.G., Wang, H., Li, D.X., Wang, X.K., 2016. Statistical analysis of turbulent super-streamwise vortices based on observations of streaky structures near the free surface in the smooth open channel flow. Water Resources Research, 52, 3563–3578.
Zhong, Q., Chen, Q., Chen, H., Li, D.X., 2017. A topological method for vortex identification in turbulent flows. Fluid Dynamics Research, 49, 015509.
Zhou, J., Adrian, R.J., Balachandar, S., Kendall, T.M., 1999. Mechanisms for generating coherent packets of hairpin vortices in channel flow. Journal of Fluid Mechanics, 387, 353–396.

Received 3 September 2019
Accepted 28 April 2020